*Physics in Canada*, **50** 9 (1994)

# Experiments with Patterns in Convecting Gases

Stephen W. Morris*,

Eberhard Bodenschatz†,

John R. de Bruyn‡

(May 20, 1996)

## I. PATTERNS: STRUCTURE FROM INSTABILITY

Physics traditionally deals with systems in equilibrium for the very good reason that they often have a high degree of symmetry and order, and hence simplicity. These features emerge because equilibrium is an optimal, limiting state; the minimum of the systems' free energy, for example. Equilibrium is, by definition, stable against small perturbations. In contrast, systems driven far from equilibrium are not so constrained; in general, they are in no stable optimum state, and indeed there may be no well-defined global function to optimize. Their dynamic behaviour may depend on their whole history. Nonequilibrium systems are usually associated with unstable, turbulent, complex behaviour. It may come as a surprise then, that there also exist nonequilibrium states which are nevertheless highly ordered, provided the system is not driven too hard. These states occupy the middle ground between order and chaos, where nonlinearity conspires to produce regular *patterns* which obey relatively simple dynamics [1]. Typically, such patterns emerge just above the threshold of an instability at which a spatially uniform state becomes unstable to perturbations near some special wavelength. These perturbations grow until they are saturated by nonlinear effects, leaving a regular, or nearly regular, stable pattern. Examples of such patterns are seen everywhere in nature, from clouds lined up in "streets" to sand ripples to the stripes

on zebras. Farther from equilibrium, patterns often display chaotic dynamics of increasingly complexity, leading eventually to featureless, turbulent behaviour. This article will describe a series of experiments on a particular pattern forming system, Rayleigh-Bénard convection, which allows highly controlled laboratory studies of stable patterns and their transition to chaos [2–4].

## II. RAYLEIGH-BÉNARD CONVECTION

Thermal convection is to pattern formation what the hydrogen atom is to quantum mechanics: the paradigm case. First studied experimentally by Bénard at the turn of the century [5], it was analysed by Lord Rayleigh [6] in 1916. He considered the stability of a fluid confined between two infinite, flat, horizontal plates separated by a distance $d$. The plates have uniform temperatures $T_1$ and $T_2$. The difference $\Delta T = T_2 - T_1$ is maintained between them, with the lower plate warmer. Lord Rayleigh showed that the motionless fluid is unstable to overturning convection when a certain dimensionless number $R$, now called the Rayleigh number, exceeds a critical value $R_c$, where

$$R = \left[\frac{g\alpha}{\kappa\nu}\right]\Delta T d^3, \tag{1}$$

and $R_c \approx 1707.26$. The quantities in square brackets are $g$, the acceleration due to gravity, $\alpha$, the thermal expansion coefficient, $\kappa$, the thermal diffusivity and $\nu$, the kinematic viscosity; all of these are constants or fixed fluid properties.

The Rayleigh number can be thought of as a dimensionless measure of the temperature difference $\Delta T$. When $R < R_c$, the fluid is motionless and transports heat only by conduction. When $R > R_c$, the fluid begins to flow and eventually arranges itself in a more-or-less ordered pattern of convection cells. The flow is driven, against viscous losses, by the buoyancy forces on the fluid, due to its thermal expansion. Note that the critical temperature difference $\Delta T_c$ required to start convection in a particular layer increases as the inverse *cube* of the thickness $d$.

For our purposes, it is more convenient to speak in terms of the *reduced* Rayleigh number $\epsilon$, given by

$$\epsilon = \Big[\frac{R}{R_c}\Big] - 1, \tag{2}$$

so that $\epsilon = 0$ at the onset of convection. As the notation implies, we will usually be concerned with small values of $\epsilon$. Experimentally, it is the temperature difference $\Delta T$ across the layer that is varied, with the other quantities in Eqn. [1] fixed, so that

$$\epsilon = \Big[\frac{\Delta T}{\Delta T_c}\Big] - 1. \tag{3}$$

Just above onset, the simplest situation occurs when $\Delta T_c$ is not too large. In this case the fluid equations simplify considerably because one can make the *Boussinesq* [7] approximation in which the temperature dependent fluid parameters $\alpha$, $\kappa$ and $\nu$ are assumed to be constant over the layer. The system then exhibits an up/down symmetry and, for a horizontally unbounded layer, the flow cells take the form of long, time-independent straight rolls. The lateral spacing of the rolls is approximately $d$. At onset, the rolls may appear in any orientation. The instability spontaneously breaks the isotropic rotational symmetry of the layer about its normal. The magnitude of the flow velocity in the convection pattern is found to grow continuously from zero above $\epsilon = 0$. This is known as a *supercritical bifurcation*, and is formally very analogous to a second order phase transition.

The situation is more interesting for the general case when the critical temperature difference $\Delta T_c$ is sufficiently large that the temperature dependances of the fluid properties cannot be neglected. A theory of the non-Boussinesq case, due to Busse [8], takes into account only the first order linear temperature dependances. He showed that the up/down symmetry of the Boussinesq case is broken, and that the flow pattern just above onset consists of hexagonal cells which appear with a jump to nonzero flow amplitude at $\epsilon = 0$. In some fluids, including most gases, the warm fluid rises around the edge of each convection cell while the cool fluid descends in the centre, while in other fluids the reverse is true. Which occurs depends on the sign of certain temperature derivatives of the fluid parameters. Near

onset there is a narrow hysteresis loop within which the hexagonal flow persists slightly below $\epsilon = 0$ for decreasing $\epsilon$. This behaviour, known as a *transcritical bifurcation*, is analogous to a first order phase transition. As $\epsilon$ is increased, Busse's theory predicts a region of bistability, in which both straight rolls and hexagonal cells are stable, followed by a regime of straight rolls as in the Boussinesq case. The point where hexagonal cells lose stability to rolls is an interesting example of a pattern-to-pattern transition.

One important difference between experiments and the theory just outlined is that the theory presumes a horizontally infinite fluid layer, while experiments are, of course, finite. The horizontal scale of an experiment is characterized by the *aspect ratio*

$$\Gamma = r/d, \tag{4}$$

where $r$ is the radius of the circular experimental fluid layer and $d$ is its thickness. In a small experiment, $\Gamma \approx 1$, the boundaries dominate and the pattern is so constrained that it loses all its spatial degrees of freedom. At higher $\epsilon$, the chaos that eventually ensues is entirely in the remaining temporal behaviour. This is a classic system for the study of "low-dimensional" dynamical chaos, of the sort found in systems of coupled nonlinear ODEs. Experiments of this kind were the first to observe experimentally the period-doubling route to chaos [9]. We are concerned here with the opposite limit, $\Gamma \to \infty$. In this limit, patterns have room to adjust themselves on scales much longer than their periodicity and may be described by, for example, slowly varying envelope approximations which take the form of PDEs in space and time. Such patterns may develop what has been called *spatio-temporal* chaos [1], which is far less understood than purely temporal chaos and is a subject of forefront interest at the present time. We shall see below that even when $\Gamma$ is quite large, the overall pattern may be strongly affected by the boundary conditions at the sidewalls.

## III. EXPERIMENTS IN CONVECTING GASES

The convecting fluid used in our experiments [2–4] was $CO_2$ gas under 20 to 30 times atmospheric pressure. There are several practical reasons why a pressurized gas is preferable

to an ordinary liquid, like water. In the first place, one can to some extent select the properties of the working fluid by varying the pressure. It also happens that the properties of $CO_2$ are very well known and favourable for reaching large $\Gamma$ because $d$ can be made quite small for reasonable values of $\Delta T_c$ and pressure. It is also important that the characteristic time scale for convection, the vertical thermal diffusion time $\tau = d^2/\kappa$, is only about $1s$ for gases, versus about $30s$ for water. $\tau$ is of order the turnover time of a convection cell. This small $\tau$ makes it experimentally possible to study patterns that have evolved long enough that they have reached their long-time limit behaviour. The time scale to reach this limit is of order the horizontal thermal diffusion time $\Gamma^2\tau$, which was a only a few hours in our gas experiments.

One might wonder whether the compressibility of the gas needs to be taken into account: the theory outlined above assumed incompressible flow. This depends on the Mach number $M$, which is the ratio of the typical flow velocity to that of sound. Compressibility is important when $M \approx 1$, whereas for our flows $M \approx 10^{-6}$ and incompressibility is an excellent approximation.

Another property of gases which makes them very interesting for convection experiments is captured by yet another dimensionless parameter, the Prandtl number

$$\sigma = \nu/\kappa. \tag{5}$$

The Prandtl number is a dimensionless measure of the relative rates of diffusion of temperature (via $\kappa$) and momentum (via $\nu$). Viscous fluids with poor thermal conductivity, such as silicone oil or the rock in the Earth's mantle, have a large $\sigma$, while thin fluids with high thermal conductivity, like liquid helium or mercury, have a small $\sigma$. Water has $\sigma = 5$ to 10, depending on temperature. Certain terms in the fluid equations scale as $\sigma^{-1}$ so that interesting new effects occur for $\sigma \leq 1$. Gases have $\sigma \approx 1$, but unlike flows in liquid helium or mercury, flow patterns in gases can be directly visualized using the shadowgraph method described below.

In order to experimentally achieve some of the degree of idealization assumed by the

theory, one must work quite hard. In particular, because $\Delta T_c \sim d^{-3}$, both the thickness of the convection volume and the temperatures must be very uniform to avoid spatial variation in $\epsilon$. A schematic of the apparatus is shown in Fig. 1. The upper side of the convection volume was formed by a single crystal sapphire $\lambda/5$ optical flat, while the bottom side was an aluminum [3] (in some experiments silver [2] ) plate which was diamond machined to $\lambda/2$. The spacing between the plates $d$ was about $500\mu$m, and uniform to within $1\mu$m. In some experiments this was done with a rigid ceramic spacer [2], while in others the bottom plate was positioned with three piezoelectric translators [3]. The convection volume was cylindrical with a radius $r$ of about 40mm, so that $\Gamma \approx 80$. The temperature of the bottom plate was feedback controlled to $\pm 0.5$ mK, using an embedded thermistor and a thin film heater covering its bottom surface. The top sapphire was temperature controlled by flowing water to $\pm 2$ mK, using a pump and heater arrangement. The entire experiment, including the water pump, was enclosed in a pressure vessel equipped with a window. In this way the circulating water could be kept at the same pressure as the gas inside the convection volume. This minimized the pressure differential across the sapphire top plate so that it remained optically flat. The heat pumped through the convecting gas is ultimately removed by an external cooling jacket.

To see the flow patterns produced, we made use of the *shadowgraph* technique, which has become standard in thermal convection experiments. The principle is shown schematically in Fig. 2. The small index variations across each convection cell, due to the temperature variations, act as lenses. If a parallel beam of light is passed through the convecting fluid, it will be alternately focussed and defocussed on a distant screen. In the case of our apparatus, the parallel beam is brought in through the window, the cooling water and the transparent top sapphire of the convection volume. After passing through the convecting gas, it is reflected by the mirrored bottom surface and back out of the apparatus. The reflected light is directed via some optics onto the active area of a CCD videocamera, from which an image can be periodically stored by the computer controlling the apparatus. These images, which can be quite quantitatively analysed, comprise most of the data gathered in the experiment.

In a shadowgraph image, light areas correspond to cool upflowing fluid and the dark areas to warm, downflowing fluid. The images are recorded using an 8-bit greyscale and divided by reference images with no convection; the results presented here have been thresholded for the purposes of presentation.

## IV. HEXAGONS AND SPIRALS IN NON-BOUSSINESQ CONVECTION

The first experiments with this apparatus [2] were studies of non-Boussinesq convection. This pattern system had previously only been studied in rather small aspect ratios ($\Gamma \approx 20$), and the hysteresis at onset had only been studied by global heat flow measurements. In our experiments, the pressure was chosen such that $\Delta T_c$ was $29^oC$. Even with this rather large $\Delta T_c$, the hysteresis loop only spans an epsilon range of about $2 \times 10^{-3}$. Fortunately, the precise control of $\Delta T$ and the large value of $\Delta T_c$ combine through Eqn. [3] to give an experimental resolution in $\epsilon$ of about $3 \times 10^{-5}$. It was found that the hexagonal flow cells appear at a special point in the convection volume and quickly increase to finite amplitude, forming a growing patch. This process appears to be very analogous to heterogeneous nucleation. Because the cell is not perfect, $\Delta T$ and $d$ vary slightly from place to place. Convection is nucleated at the point in the cell where $R \sim \Delta T d^3$ is largest, and hence the point where $\epsilon$ crosses through zero first. Once started, convection grows by front propagation, just as does nucleation at a first order phase transition. Over a narrow range of $\epsilon$, the pattern grows to take over the whole convection volume. Fig. 3 shows the resulting perfect "crystal" of hexagonal flow cells. The lattice may appear with any orientation - again, this is a symmetry breaking transition. This pattern is a striking example of an ordered state that emerges only under nonequilibrium conditions. The flow is dissipative because the gas has viscosity; this pattern, like the reader of this page, is continuously producing entropy which is exported to the environment.

As $\epsilon$ is slowly increased, theory predicts a regime of bistability near $\epsilon \approx 0.1$, where both hexagonal and straight roll flow cells are stable, but that there should be no transition

between them. What was found experimentally was different and unexpected. Another nucleation-like transition was found in the range where only bistability was expected. Rolls, which nucleate at the sidewalls, invade the hexagonal pattern and eventually fill the convection volume. But they are neither straight, nor stationary. Fig. 4 shows a snapshot of one pattern that is found. It is a periodic, rotating, one-armed spiral composed of curved rolls. The roll which forms the spiral arm ends in the central core and at a dislocation which occurs about halfway along the radius. Beyond the radius of the dislocation, the roll pattern is concentric. In repeated runs, both left and right handed spirals were seen [4], as well as $n$-armed spirals with $n$ up to 13. In all cases, the sense of rotation of the spirals was such that the rolls propagated outward from the centre. The period of rotation of the spiral shown in Fig. 4 was several thousand $\tau$.

The presence of these spiral states was at first puzzling. Were they an unexpected consequence of using a non-Boussinesq fluid? The use of a ceramic spacer for the sidewall of the convection volume lead to small temperature gradients near the sides. It is well known that gradients in $\epsilon$ tend to align rolls perpendicular to the gradient. This alignment is visible even in the hexagonal flow regime, as in Fig. 3, where a few rolls are seen encircling the pattern. Are the spirals stabilized or somehow selected by these special boundary conditions? A new series of experiments was started to investigate these questions.

## V. SPIRAL DEFECT CHAOS IN BOUSSINESQ CONVECTION

The ceramic sidewall of the previous experiments was replaced with porous paper, which has thermal properties more similar to the gas. This has the effect of reducing the sidewall temperature gradients and altering the boundary conditions on the pattern. The thickness $d$ was no longer determined by a spacer, but rather by a piezoelectrically adjustable mount. The gas pressure was also increased, making the system more Boussinesq; $\Delta T_c$ was reduced to about $6^oC$. In place of the hexagonal pattern, the expected time-independent straight rolls are seen just above onset, as shown in Fig. 5. Notice that the rolls are straight, even

though the cell is round. The lateral boundary conditions now favour rolls perpendicular to the sides. The pattern initially accomplishes this by forming small grain boundaries at its edge. As $\epsilon$ is increased, the orienting effect of the sidewalls increases and one observes frustrated patterns of the kind shown in Fig. 6. The pattern is dominated by a few *focus* singularities around the perimeter which are centres for patches of concentric rolls. These patches meet at slowly moving grain boundaries. The pattern is frustrated because no straight roll solution is available that satisfys the circular boundary conditions.

At $\epsilon \approx 0.5$ rotating spiral defects begin to appear in the centre of the pattern as in Fig. 7. Eventually, around $\epsilon \approx 1$ the convection volume is filled with a chaotic mass of interacting rotating spiral defects, as in Fig. 8. We have called this state *spiral defect chaos*. It is chaotic in the strong sense of spatio-temporal chaos, in which the system displays complexity in both space and time. We subsequently found that this state is reached at higher $\epsilon$ values under both Boussinesq and non-Boussinesq conditions, and for either sort of boundary conditions.

Locally, the flow is still very similar to that of a straight roll, the complex time dependence is due to the appearance, motion and disappearance of defects in the roll pattern. This is an example of *weak* or *defect* turbulence [1]. This very simple type of turbulence does not have the cascade of length scales that one associates with ordinary featureless turbulence. One can measure some statistical properties of this chaotic state, such as the correlation length $\xi$, which is a measure of the mean size of patches of rolls or spirals. It was found [3] that $\xi(\epsilon)$ scales very nearly as $\epsilon^{-1/2}$. At present this power-law behaviour remains unexplained. For $\epsilon \approx 1$, the chaotic system is *large* in the sense that size of a correlated region becomes very small compared to the size of the whole pattern.

The chaotic state is found in regimes where theory for a laterally infinite layer has shown that straight rolls are a stable state [10]. It seems likely, in view of its "large" character, that the spiral defect chaotic state is another possible solution for the infinite layer, and one which is reached from the range of initial conditions which is accessible by the experiment. Unfortunately, it is not currently understood how to extend the familiar phase space concepts of a chaotic attractor and its basin of attraction, which are so useful in the phenomenology

of low dimensional chaos, to the general case of spatio-temporal chaos.

## VI. CONCLUSION

The spirals and other patterns we observe in Rayleigh-Bénard convection have stimulated several large scale numerical simulations [11–13] of nonlinear PDE model equations. These model equations, which are based on the *Swift-Hohenberg* equation [1], represent an enormous simplification over the full fluid mechanical equations of the problem. Nevertheless, it is still a formidable task to numerically integrate them. They contain only the lowest order nonlinear terms required by symmetry, yet they capture the essence of the phenomena. It has been found that one must include certain *mean flow* [14] terms in order to account for the rotating spirals and chaotic state that we observed. These very small flows move in the horizontal plane of the convection volume and have length scales much larger than the roll spacing; they are not visualized by the shadowgraph. Specifically, the simulations show that there is a vortex of mean flow associated with each spiral or spiral patch. The circulation of the mean flow carries the rolls along, bringing about the rotation of the spirals. Conversely, the *curvature* of convection rolls acts as a source term of the pressure field that drives the mean flow. These effects are only important for fluid with Prandtl numbers $\sigma <\approx 1$, which is the case for our gas. Thus, the simulations give us a qualitative sense of the physics underlying the experimental results. There are, however, many open questions. The role of noise during the pattern transformations and the sensitivity of the chaotic state to noise remain uninvestigated. We have no quantitative understanding of spatio-temporal chaos in general, or of the spiral chaos state in particular. The field of nonequilibrium patterns is young and growing.

## ACKNOWLEDGMENTS

This work was done in collaboration with Guenter Ahlers and David Cannell while the authors were postdoctoral fellows at The University of California, Santa Barbara. No mere ac-

knowledgement can express our thanks. S. W. M. and J. R. de B. were supported by NSERC, and E. B. was supported by the Deutsche Forschungsgemeinschaft. The experiments were supported by the U.S. Department of Energy through grant DE-FG03-87ER13738.

# REFERENCES

* Department of Physics and Erindale College, University of Toronto.

† Department of Physics, Cornell University.

‡ Department of Physics, Memorial University.

[1] This field has recently been very extensively reviewed; see M. C. Cross and P. C. Hohenberg, *Rev. Mod. Phys.*, **65**, 851 (1993), and the references therein.

[2] E. Bodenschatz, J. R. de Bruyn, G. Ahlers and D. S. Cannell, *Phys. Rev. Lett.*, **67**, 3078 (1991).

[3] S. W. Morris, E. Bodenschatz, D. S. Cannell and G. Ahlers *Phys. Rev. Lett.*, **71**, 2026 (1993).

[4] E. Bodenschatz, S. W. Morris, J. R. de Bruyn, D. S. Cannell and G. Ahlers, *Phys. Fluids A*, **5**, S8 (1993).

[5] H. Bénard, *Ann. Chim. Phys.*, **7** (ser. 23), 62 (1900).

[6] Lord Rayleigh, *Proc. R. Soc.* (London), **93** (ser. A), 148 (1916).

[7] More correctly, this is should be called the "Oberbeck-Boussinesq" approximation.

[8] F. H. Busse, *J. Fluid Mech.*, **30**, 625 (1967).

[9] A. Libchaber and J. Maurer, *J. Phys.* (Paris), **C3**, 51 (1980).

[10] R. M. Clever and F. H. Busse, *J. Fluid Mech.*, **65**, 625 (1974), and F. H. Busse and R. M. Clever, *J. Fluid Mech.*, **91**, 319 (1979).

[11] H. Xi, J. D. Gunton and J. Viñals, *Phys. Rev. E*, **47**, R2987 (1993).

[12] M. Bestehorn, M. Fantz, R. Friedrich and H. Haken, *Phys. Lett. A*, **174**, 48 (1993).

[13] H. Xi, J. D. Gunton and J. Viñals, *Phys. Rev. Lett.*, **71**, 2030 (1993).

[14] E. D. Siggia and A. Zippelius, *Phys. Rev. Lett.*, **47**, 835 (1981).

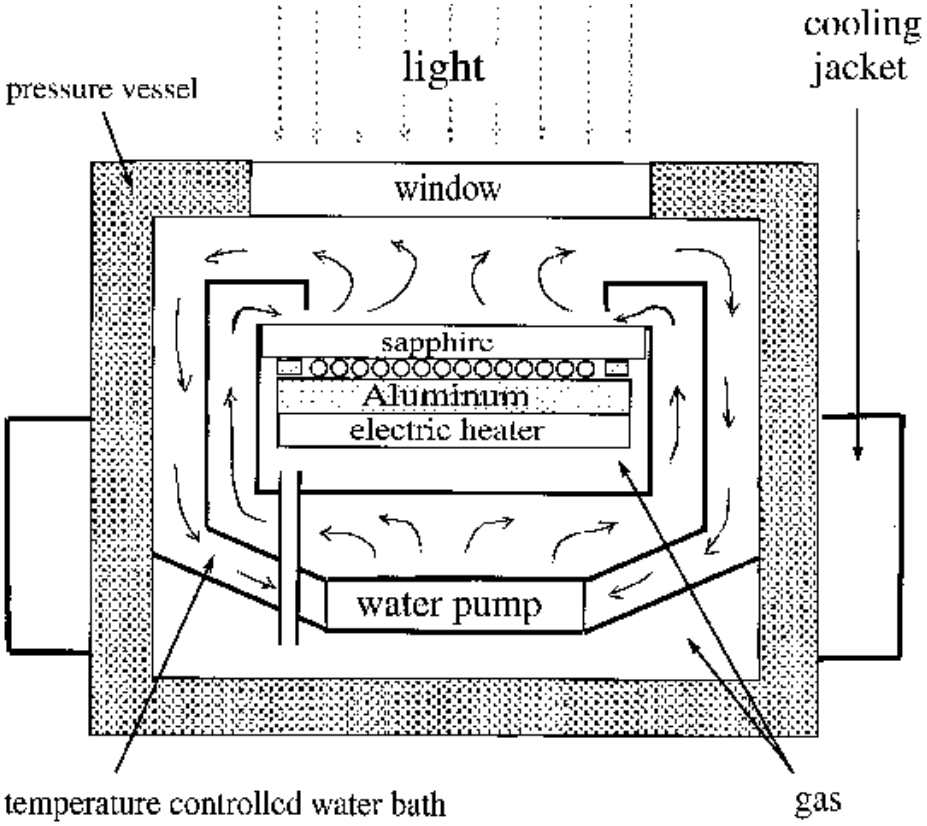


FIG. 1. A schematic drawing of the gas convection apparatus.

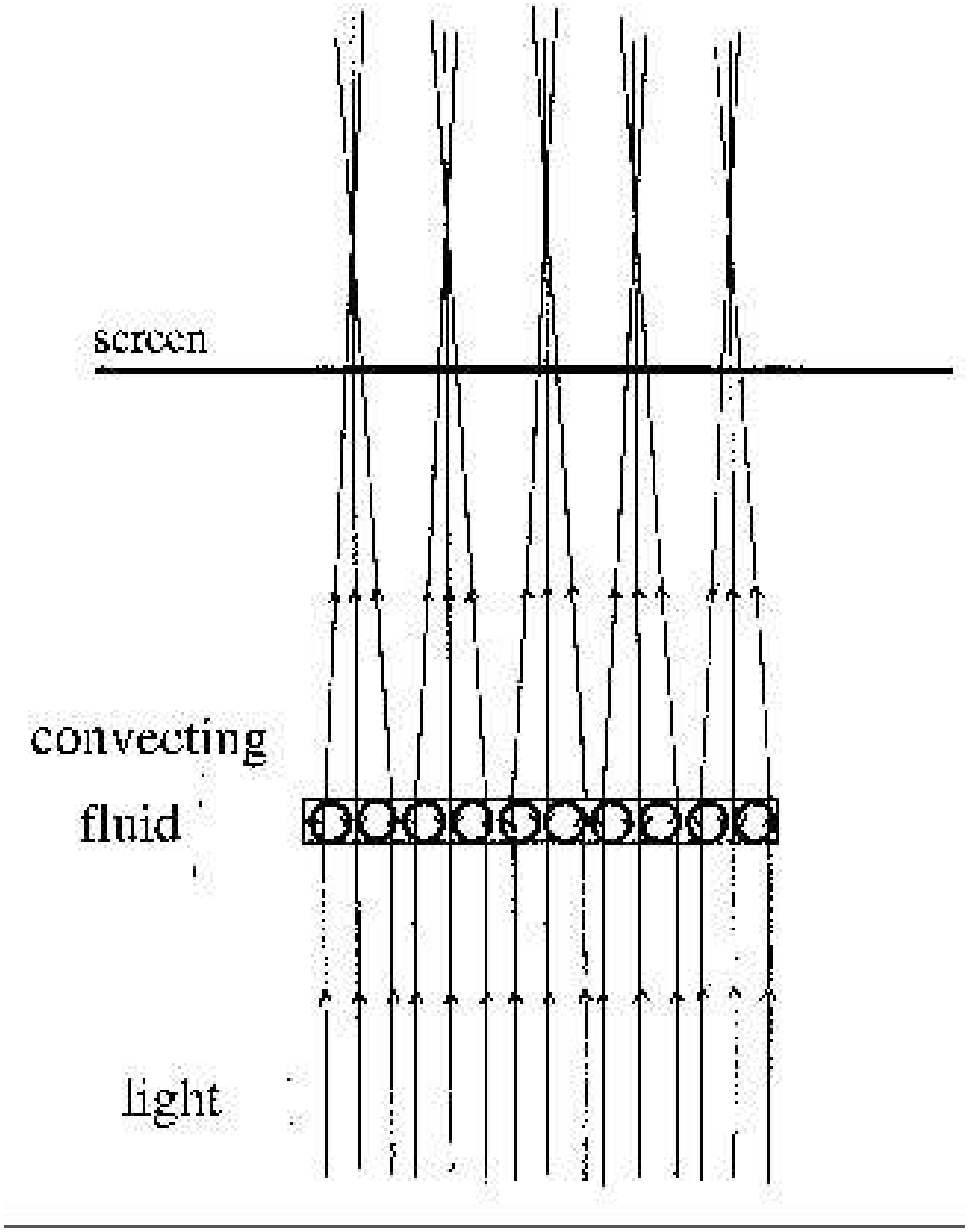


FIG. 2. A schematic diagram of the shadowgraph method for visualizing convection patterns.

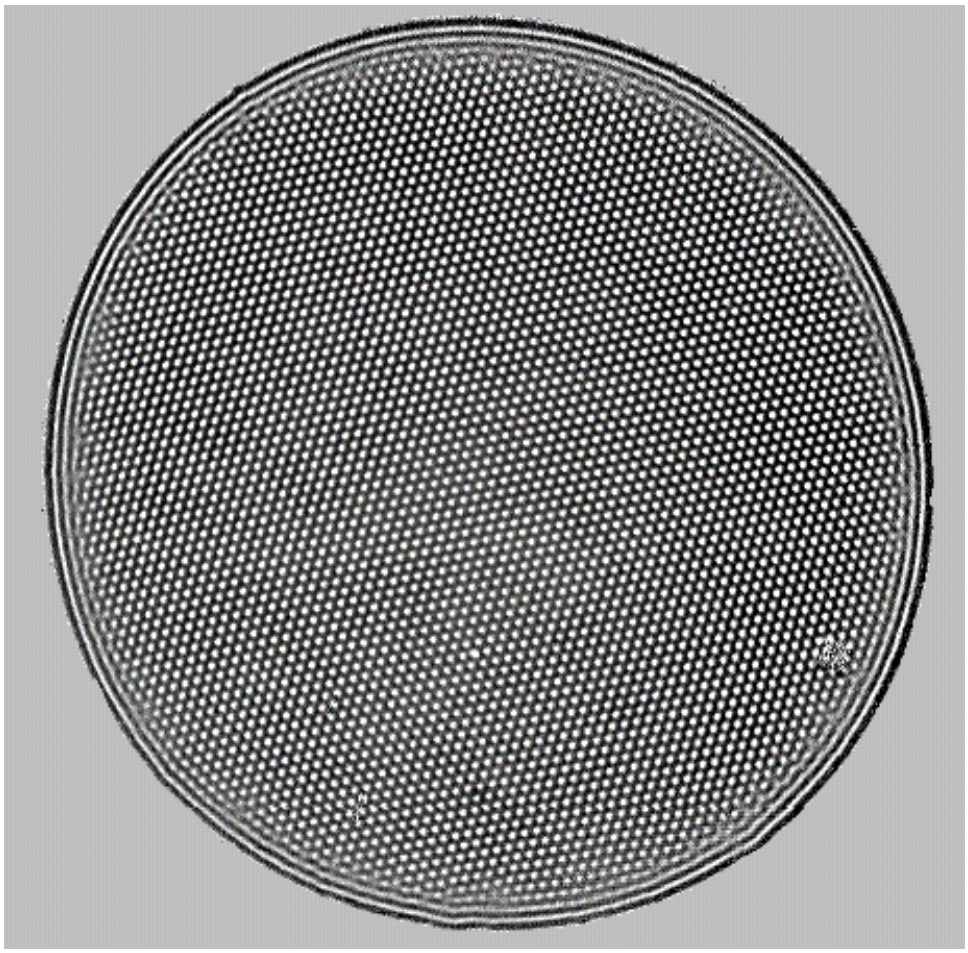

FIG. 3. The convection pattern just above onset under non-Boussinesq conditions. $\epsilon \approx 0.06$.

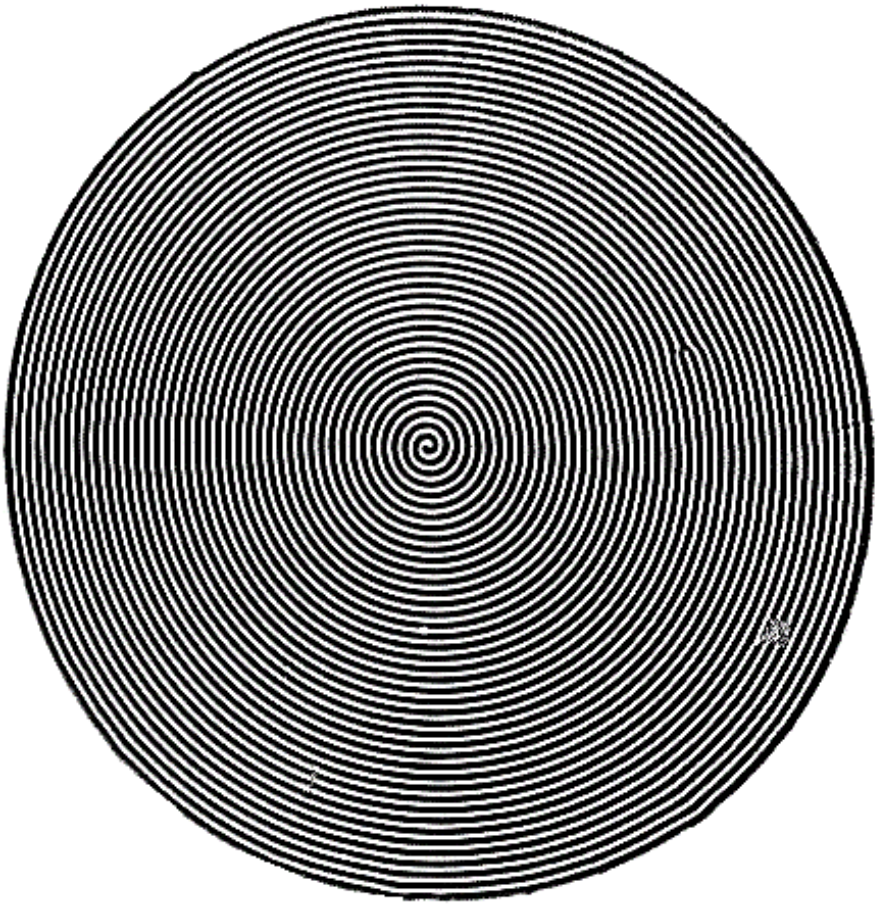

FIG. 4. A rotating one-armed spiral pattern seen under non-Boussinesq conditions. $\epsilon \approx 0.1$.

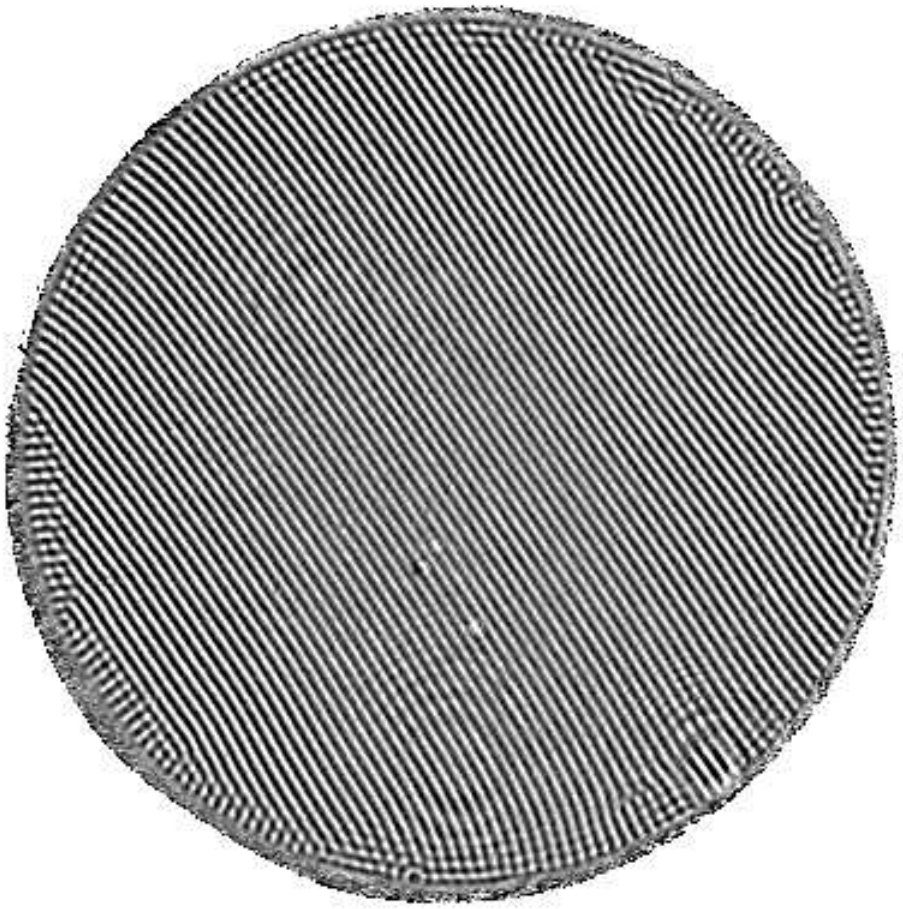

FIG. 5. Straight convection rolls seen just above onset under Boussinesq conditions. $\epsilon \approx 0.04$.

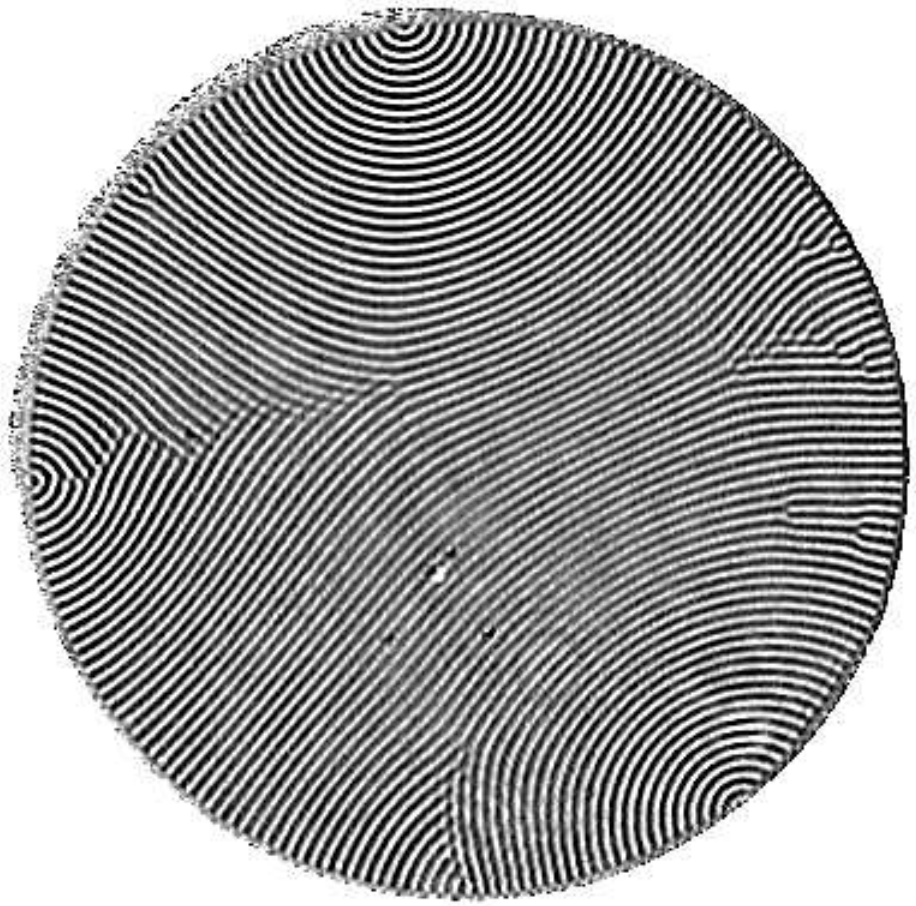

FIG. 6. A frustrated pattern in which the rolls curve to meet the sidewall boundary conditions. $\epsilon \approx 0.1$, Boussinesq conditions.

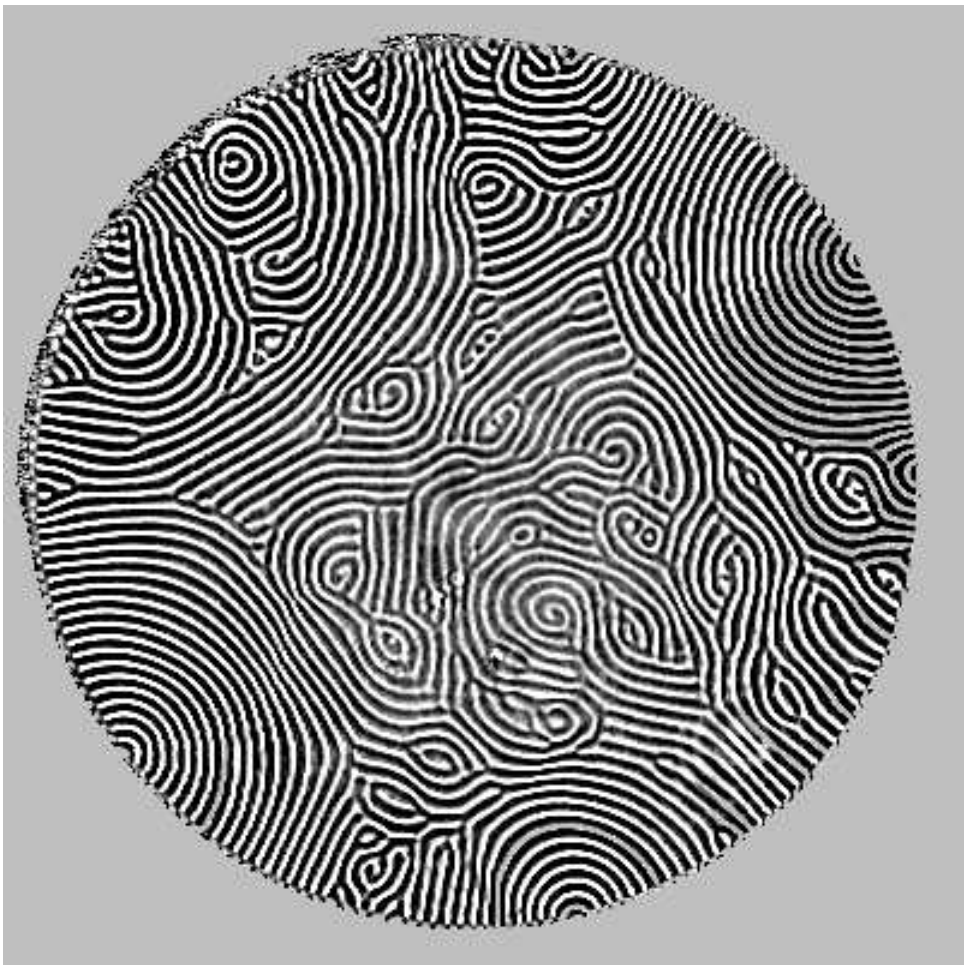

FIG. 7. At increased $\epsilon$, rotating spiral defects appear under Boussinesq conditions. $\epsilon \approx 0.5$.

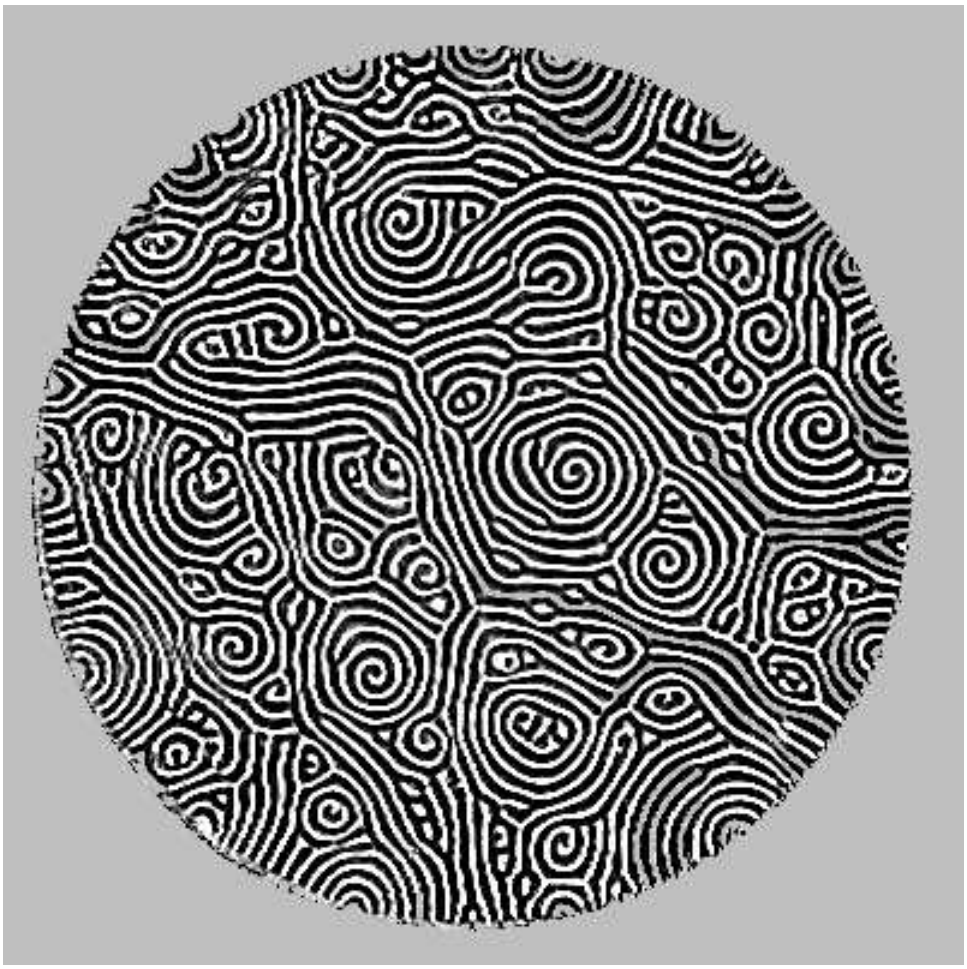

FIG. 8. Spiral defect chaos eventually fills the whole convection volume. $\epsilon \approx 0.7$, Boussinesq conditions.